

Investigation Fiber Laser Effects on Titanium Gr2: Color marking and Surface Roughness

Jēkabs Lapa

Rezekne Academy of Technologies
Faculty of engineering
Rēzekne, Latvia
jekabs.lapa@gmail.com

Imants Adijāns

Rezekne Academy of Technologies
Faculty of engineering
Rēzekne, Latvia
imants.adijans@rta.lv

Emil Yankov

Rezekne Academy of Technologies
Faculty of engineering
Rēzekne, Latvia
emil.yankov@rta.lv

Lyubomir Lazov

Rezekne Academy of Technologies
Faculty of engineering
Rēzekne, Latvia
lyubomir.lazov@rta.lv

Ritvars Rēvalds

Rezekne Academy of Technologies
Faculty of engineering
Rēzekne, Latvia
ritvars.revalds@rta.lv

Abstract. In this subsequent investigation, we expand upon our initial research by delving into the laser engraving and marking of Grade 2 Titanium (Ti Gr 2) using frequencies of 300 kHz and 700 kHz. Building upon our preliminary experiments involving 100 kHz and 500 kHz, we utilized the Rofin PowerLine F 20 Varia fiber laser to mark Grade 2 titanium within a 6x6 matrix, with each square measuring 5x5 mm. Our meticulous adjustments to the laser marking parameters — encompassing speed (100-1100 mm/s), power (8-18 W), and the introduction of new frequencies (300 kHz and 700 kHz) — allowed us to scrutinize their impact on surface roughness and contrast. Employing advanced techniques, including a laser scanning microscope and Adobe Photoshop software, our analysis unveiled explicit connections among contrast, roughness, frequency, scanning speed, and power. These findings not only extend the scope of our previous experiments but also illuminate subtleties specific to the 300 kHz and 700 kHz frequencies. The insights derived from this study furnish crucial information on the optimal laser marking parameters for Grade 2 titanium, thereby augmenting its efficacy and durability across a diverse array of applications. Moreover, this research contributes to the progressive comprehension of color variations in laser-engraved titanium Grade 2, particularly within the 300 kHz and 700 kHz frequency range.

Keywords: Fiber laser, laser color marking, laser texturing, titanium Gr2.

I. INTRODUCTION

In the ever-evolving landscape of materials processing, lasers have emerged as transformative tools, revolutionizing traditional methodologies over the past two decades. Known for their precision, heightened productivity, and cost efficiency, lasers have become

integral across various industries. Laser processing, encompassing activities from marking and texturing to welding, stands at the forefront of material transformation, impacting metals and nonmetals alike.

Laser applications have witnessed a surge in popularity [1], finding diverse applications in marking [2], texturing [3], welding, and material treatment across both metallic and non-metallic substrates [4], [5]. When juxtaposing laser-induced marking and texturing against alternative techniques such as pattern marking systems, abrasive etching [6], and others, the distinctive advantages of laser methodologies [7] become readily apparent. These include exceptional swiftness in marking, unmatched precision, and the elimination of the need for subsequent post-treatment steps. Currently, a wealth of academic explorations and research pursuits dive into the expansive domain of laser processing, encompassing a diverse spectrum of materials like titanium [8].

Particularly notable is the scientific quest to unveil new hues on titanium surfaces [9], through the interplay of laser irradiation and infrared temperature measurements. The process of transforming the color of titanium with a laser involves the intentional development of oxidation layers or structures on the material's surface [10]. This purposeful manipulation induces thin-layer diffraction, culminating in a noticeable transformation of color [11].

Several investigations have delved into the realm of laser color marking on metals [12]. The pursuit of desired colors necessitates meticulous control over the thickness of the thin film oxide layer. Recent

Print ISSN 1691-5402

Online ISSN 2256-070X

<https://doi.org/10.17770/etr2024vol3.8167>

© 2024 Jekabs Lapa, Imants Adijāns, Emil Yankov, Lyubomir Lazov, Ritvars Rēvalds.

Published by Rezekne Academy of Technologies.

This is an open access article under the [Creative Commons Attribution 4.0 International License](https://creativecommons.org/licenses/by/4.0/).

advancements underscore the capability of nanosecond fiber lasers to generate oxide layers on titanium surfaces within ambient atmospheric conditions [13], leading to dynamic color transformations. These breakthroughs significantly contribute to the evolving landscape of material processing methodologies. The significance of textured surfaces extends notably to the maritime industry, where enhanced durability against environmental stressors is crucial. Additionally, these textured surfaces find applications in the aviation sector [14], contributing to the development of heat-resistant coatings for spacecraft during atmospheric re-entry [15]. This versatility further expands their utility in aviation and maritime contexts, where the benefits of texturing are leveraged to optimize performance and ensure long-term colorfastness and resilience.

The objective of this investigation is to unveil the intricate dynamics governing the impact of power, frequency, and scanning speed, key parameters associated with a pulsed (ns) fiber laser with a wavelength of 1064 nm, on the outcomes of laser marking and texturing processes [16] applied to Grade 2 titanium. The findings contribute valuable insights to the evolving landscape of laser materials processing [17], further enhancing our understanding of optimal conditions for these surface modification techniques and their used laser parameters to achieve the desired color and texture changes.

II. MATERIALS AND METHODS

A. Sample Characteristics

This study focused on an experimental examination involving a titanium Grade 2 sheet specimen, characterized by its chemical composition: Ti (titanium) concentration $\geq 98.9\%$, Fe (iron) content $\leq 0.30\%$, O (oxygen) levels $\leq 0.25\%$, C (carbon) presence $\leq 0.080\%$, N (nitrogen) trace amounts $\leq 0.030\%$, and H (hydrogen) minimal content $\leq 0.015\%$. The physical dimensions of the specimen measured 100x100x1 mm. Prior to the commencement of the experiments, the sample surfaces underwent a meticulous purification process utilizing (C3H7OH) to eliminate any contaminants or potential blemishes.

B. Laser setup

The laser experimentation utilized the Rofin PowerLine F-20 Varia pulsed fiber laser system, as illustrated in Figure 1. Operating at a wavelength of 1064 nm, the laser demonstrated a maximum power of 19 W, and its pulse duration could be adjusted. The focusing mechanism employed a 160 mm lens, resulting in a 40 μm spot size. Laser control was facilitated through a computer-managed Galvano scanner, offering a scan field of 120x120 mm.



Fig. 1. Fiber laser Rofin PowerLine F-20 Varia.

Specification for Rofin PowerLine F-20 Varia laser is shown in Table I.

TABLE I. PARAMETERS OF ROFIN POWERLINE F-20 VARIA

Parameter	Magnitude, Unit
Wavelength (λ)	1064 nm
Max. Power (P)	19 W
Max. Pulse Energy (E)	1 mJ
Scan Speed (v)	1 mm/s to 20000 mm/s
Pulse Width (τ)	4 ns to 200 ns
Repetition Rate (F)	20 kHz to 1000 kHz

C. Microscope setup

To scrutinize the surface characteristics and alterations in the titanium Grade 2 (Ti Gr2) samples, an Olympus LEXT OLS5000 3D Measuring Laser Microscope was employed, as depicted in Figure 2. The microscope operated at a magnification of x451, ensuring a measurement precision of 0.4 μm . Additional specifications comprised a numerical aperture (N.A.) of 0.6, a working distance (W.D.) of 1 mm, a focal depth of 1.8 μm , a focusing spot diameter of 0.82 μm , covering a measurement area of 640 X 640 μm .



Fig. 1. Olympus LEXT OLS5000 3D Measuring Laser Microscope.

D. Scanner

Marked titanium Gr2 plates were scanned using an HP Scanjet G3010 scanner with a scanning area of 216 X 297 mm and a color depth of 48-bit. The scanning parameters were set to a resolution of 2400 DPI, brightness of 100, contrast of 80, and the file format used was .tif.

E. Experimental Method

Laser marking was performed on a Ti Gr 2 sample measuring 100x100x1 mm using a fiber laser. To ensure a clean surface for marking, the sample underwent thorough cleaning with isopropyl alcohol 99.8% (IPA) to eliminate any potential contaminants. The sample was marked with two matrices, each consisting of 6 rows and 6 columns, resulting in a total of 72 markings. Different combinations of speed, power, and frequency parameters were used for marking, while maintaining a constant pulse duration of 4 ns. The experiments were conducted in ambient conditions without the use of any assist gases. The marking of the Ti Gr 2 plate involved variations in three key parameters: power (P) in watts, scanning speed (v) in mm/s, and frequency (F) in kHz. Figure 3 illustrates the marking schematics of the Ti Gr 2 samples.

The marking process in the current experiment involved two matrices, each defined by specific parameters shown in Table II. For marking the first matrix, a frequency of 300 kHz was used. For marking the second matrix, a frequency of 700 kHz was used. This adaptation aims to explore the laser marking process comprehensively, particularly focusing on the effects under the influence of different frequency settings with constant pulse duration.

TABLE II. FIBER LASER MARKING PARAMETERS FOR Ti Gr 2 SHEET SAMPLE AT 300 KHZ AND 700 KHZ

Parameter	Magnitude, Unit
Pulse Duration (τ)	4 ns
Output Power (P)	8/10/12/14/16/18 W
Scanning Speed (v)	100/300/500/700/900/1100 mm/s
Square Size	5×5 mm
Frequency (F)	300 kHz and 700 kHz

Equation (1) was used to convert the laser power from % to W.

$$P(W) = \frac{19 * P(\%)}{100\%} \quad (1)$$

Here, $P(W)$ = laser power in W, and $P(\%)$ = signifies laser power in %. The resulting power values in watts, corresponding to the power percentages, are presented in Table III.

TABLE III. POWER CONVERSION CHART

$P(\%)$	41.7	52.1	62.5	72.9	83.3	93.8
$P(W)$	8	10	12	14	16	18

To compute the contrast factor, denoted as k_x , a percentage value is employed [18]. The determination of k_x involves assessing the volume N_f , of the unmarked region [19]. Conversely, the N_x value pertaining to the laser-marked region is directly derived from the marked area. The formula utilized for the calculation of k_x is expressed in Equation (2):

$$k_x = \frac{N_f - N_x}{N_f} \times 100\% \quad (2)$$

To depict the distinction between two measured colors within the CIE color uniform space, the CIE color difference $L^* a^* b^*$ formula [19], is applied. The overall color difference, N_x , [20] between two points in the three-dimensional color space is articulated using Equation (3):

$$N_x = \sqrt{(\Delta L_x)^2 + (\Delta a_x)^2 + (\Delta b_x)^2} \quad (3)$$

Similarly, the total color difference N_f is expressed using Equation (4):

$$N_f = \sqrt{(\Delta L_f)^2 + (\Delta a_f)^2 + (\Delta b_f)^2} \quad (4)$$

In these equations, ΔL , Δa , and Δb represents differences in brightness, color along one axis, and color along another axis, respectively [20]. These differences are derived from the marked areas L, a, and b using the Adobe Photoshop color tool. The L channel pertains to variations in lightness or darkness within the color spectrum.

To avoid negative contrast values, an absolute value ($|k_x|$) is applied to each calculated contrast value.

III. RESULTS AND DISCUSSIONS

The laser treatment of Titanium Grade 2 resulted in changes in contrast (color marking) and surface roughness compared to untreated material. The obtained results for the marked samples of Titanium Grade 2 can be observed in Figures 3 to 10, where the data from the conducted experiment are depicted at frequencies of 300 kHz and 700 kHz.

In Figure 3, a sample of Titanium Grade 2 plate subjected to laser treatment with a frequency of 300 kHz is depicted. As a result of this laser interaction, the pattern matrix manifested with colors, thereby creating an intriguing comparison with the matrix created using a frequency of 700 kHz, visualized in Figure 7.

Upon closer examination of the color change, various phenomena and their correlations can be observed. This color dynamics encompass transitions from green to blue, red to violet, graphite gray to gray, white to yellowish, and beige to blue. These variations in color produce a unique visual effect, providing insight into the laser impact on the surface structure of Titanium Grade 2 and the approximate color shifts it induces.

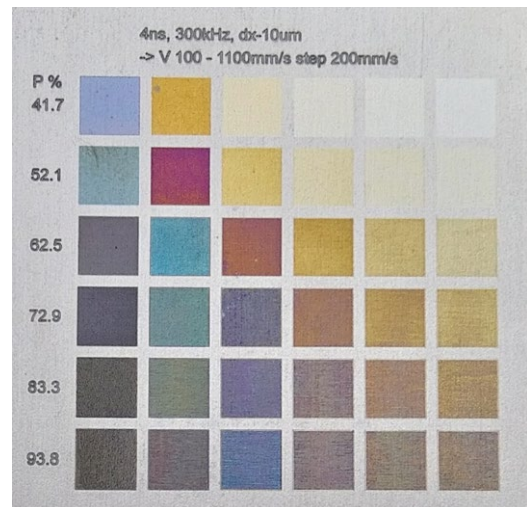


Fig. 3. Laser marked Ti Gr 2 samples with 300 kHz.

In Figure 4, surface changes are visualized by performing treatment at a frequency of 300 kHz, maintaining a constant pulse duration of 4 ns, and altering scanning speeds and laser power. The obtained absolute contrast values, calculated by considering the percentage difference between the marked and unmarked areas, provide information about the alteration in visual perception, where the contrast value N_f of the unmarked area remains constant at 75.

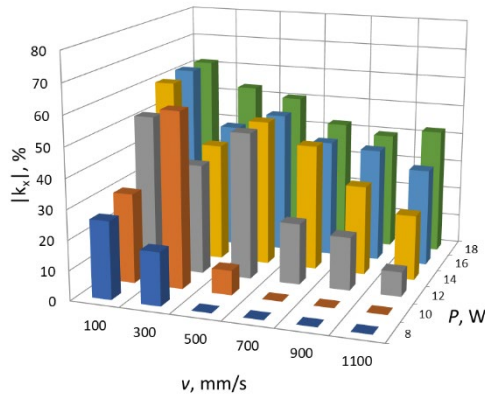


Fig. 4. Exploring the influence of scan speed, frequency (300 kHz), and power variation on the absolute contrast values in Ti Gr2 laser marking.

Delving into the laser-marked surface alterations, the scrutiny of acquired outcomes unveils a perceptible association between the established matrix and the graphical portrayal of contrast values, evident in Figures 3 and 4. Notably, the amplification in power values corresponds to a proportional surge in the absolute contrast value $|k_x|$ (%), while a simultaneous decline in $|k_x|$ values transpires with the escalation of speed values from 100 mm/s to 1100 mm/s.

A detailed examination of both visual representations highlights consistent patterns among the parameters. Adjusting power values from 8 W to 18 W at a scanning speed of 100 mm/s produces darker tones, whereas an augmentation in speed results in lighter hues. The zenith of contrast $|k_x|$ absolute values is reached at the lowest speed of 100 mm/s and the highest power of 18 W, culminating in a specific $|k_x|$ absolute value of 61.3%. Conversely, the nadir of $|k_x|$ absolute value, 1.37%, is discerned at 10 W power and a scanning speed of 700 mm/s. With an increase in scanning speed, lighter color tones emerge, appearing approximately at $|k_x|$ % values within the range of 30-50%. This phenomenon is also evident in Figure 3, specifically in the central section of the matrix, where shades of red, green, and blue begin to surface. These tones become noticeable at 10 W power and 300 mm/s scanning speed, as well as at 12-14 W power and 300-500 mm/s scanning speed.

Ti Gr 2 material surface roughness, obtained through laser marking/treatment, was analyzed using the R_q parameter. Roughness R_q of the non-marked Ti surface (Base) was measured to be $0.8 \mu\text{m}$. In Figure 5, the surface roughness of Ti Gr 2 is depicted under consistent conditions, with a 4 ns pulse duration, $10 \mu\text{m}$ marking step, 300 kHz frequency, and scanning speeds ranging from 100 to 1100 mm/s.

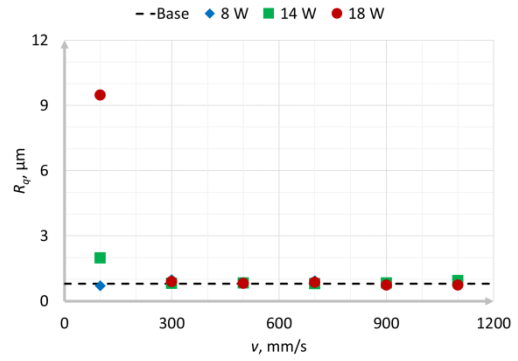


Fig. 5. Surface roughness (R_q) dependence from scanning speed for Ti Gr 2 marked samples at 300 kHz laser frequency, 4 ns pulse duration, and $10 \mu\text{m}$ marking step.

At a laser power of 8 W, R_q parameter varied from $0.70 \mu\text{m}$, achieved at a scanning speed of 100 mm/s, to the highest roughness value of $0.96 \mu\text{m}$ at a scanning speed of 300 mm/s. When comparing these results to the processing zone of 18 W power, significant differences were observed. At a scanning speed of 100 mm/s, the roughness value reached $9.5 \mu\text{m}$, while the lowest roughness value at a scanning speed of 1100 mm/s was recorded at $0.73 \mu\text{m}$. In Figure 5, we observe an increase in roughness only at speeds of 100 mm/s and power levels of 18 W and 14 W.

Figure 6 shows how roughness varies with laser power. At power 14 W, 16 W and 18 W and speed 100 mm/s, the roughness increases and reaches a maximum of $10.5 \mu\text{m}$ at 16 W and 100 mm/s. At all other combinations of power and speed, the roughness changes minimally and remains practically the same as the unmarked titanium surface (Base).

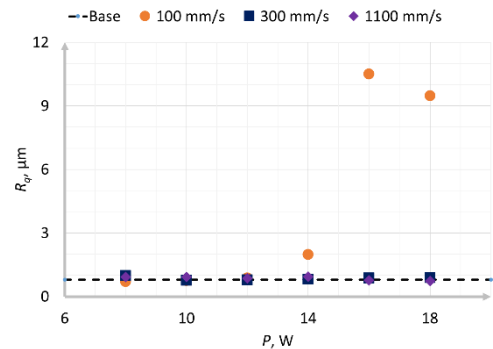


Fig. 6. Surface roughness (R_q) dependence from power for Ti Gr 2 marked samples at 300 kHz laser frequency, 4 ns pulse duration, and $10 \mu\text{m}$ marking step.

In Figure 7, the generated matrix for the Ti Gr2 sample is observed at a frequency of 700 kHz. This sample displays more vivid colors, including violet, yellow, various shades of gray, blue, and green. These distinct color tones notably contrast with the matrix colors observed at a frequency of 300 kHz, although certain areas also demonstrate a few similarities.

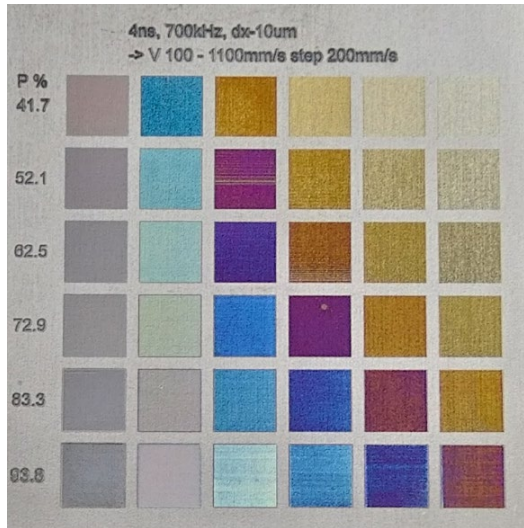


Fig. 7. Laser marked Ti Gr 2 samples with 700 kHz.

Reviewing the obtained contrast values %, at 700 kHz matrix processing, the highest contrast value is observed at 12 W power and a scanning speed of 500 mm/s, reaching a contrast value of 73.9% $|k_x|$ (see fig. 8.). Conversely, the lowest contrast value, 8.22%, was observed at 8 W power and a scanning speed of 1100 mm/s, where the color tone almost matches the sample color tone.

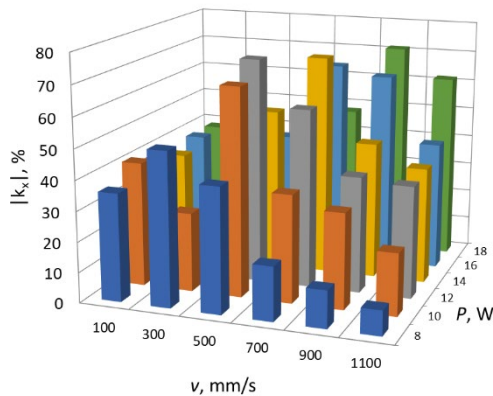


Fig. 8. Exploring the influence of scan speed, frequency (700 kHz), and power variation on the absolute contrast values in Ti Gr2 laser marking.

In Figure 9, the surface roughness of Ti Gr 2 is depicted under consistent conditions, with a 4 ns pulse duration, 10 μ m marking step, 700 kHz frequency, and scanning speeds ranging from 100 to 1100 mm/s.

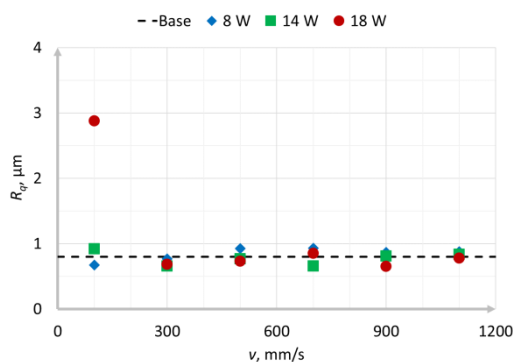


Fig. 9. Surface roughness (R_q) dependence from scanning speed for Ti Gr 2 marked samples at 700 kHz laser frequency, 4 ns pulse duration, and 10 μ m marking step.

Similar roughness characteristics are observed at a frequency of 700 kHz. The study demonstrates that the behavior of the treated surface at 700 kHz frequency is identical to that at 300 kHz frequency. At 8 W power, a slight increase in roughness is observed, starting from 0.67 μ m and increasing to 0.88 μ m proportionally with the scanning speed. However, analyzing the marking at 18 W power reveals roughness value patterns like those at 300 kHz marking but with some differences. Similar to 300 kHz, the highest roughness value starts at a scanning speed of 100 mm/s with a roughness value of 2.9 μ m, and as the scanning speed increases, the roughness value decreases to 0.8 μ m. In Figure 9, we observe an increase in roughness only at speeds of 100 mm/s and power levels of 18 W.

Figure 10 shows how roughness varies with laser power. At power 18 W and speed 100 mm/s, the roughness increases and reaches a maximum of 2.9 μ m. At all other combinations of power and speed, the roughness changes minimally and remains practically the same as the unmarked titanium surface.

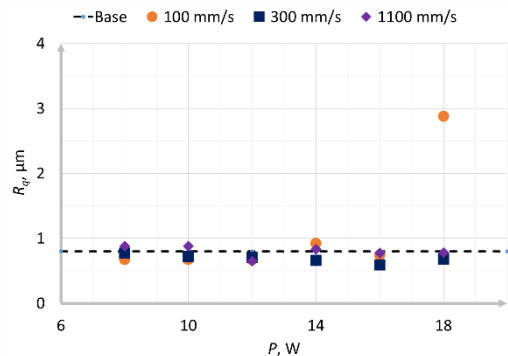


Fig. 10. Surface roughness (R_q) dependence from power for Ti Gr 2 marked samples at 700 kHz laser frequency, 4 ns pulse duration, and 10 μ m marking step.

Figure 11 shows a surface with high roughness and a dark color tone, as seen in the first column of the matrix at 93.8% power (18 W), as shown in Figure 3. Analyzing the collected data leads to the observation that rougher surfaces tend to display darker tones. However, scrutinizing the data reveals that this assertion does not consistently align with the obtained results, as evidenced by the case at 300 kHz, where the color tone in the first row at 72.9% power (14 W) is darker than at 93.8% (18 W). In this instance, the roughness value is 2.0 μ m, while the measurement at maximum power is 9.5 μ m. Uncovering correlations suggests that higher powers and lower scanning speeds result in darker tones and larger roughness. However, the color tone itself is not always a shade of black. It is conceivable that there is a relationship between roughness and color tones, but further experiments are needed to elucidate this connection.

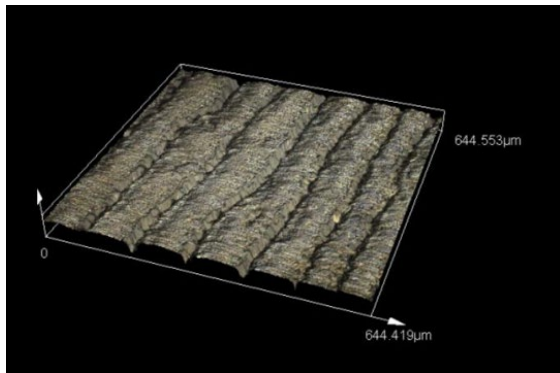


Fig. 11. Surface Roughness Analysis of Ti Gr 2 Markings at 300 kHz: 3D Laser Scanning Microscope Image (x451 Magnification) Showing $R_q = 9.5 \mu\text{m}$.

Based on our findings, the comparison of contrast values and colors revealed that at a frequency of 700 kHz, the roughest marking reached $2.9 \mu\text{m}$, as depicted in Figure 12. Figures 11 and 12 illustrates how the roughness values change while maintaining identical parameters but with a different frequency. It appears that as the frequency increases to 700 kHz, the manifestation of roughness improves.

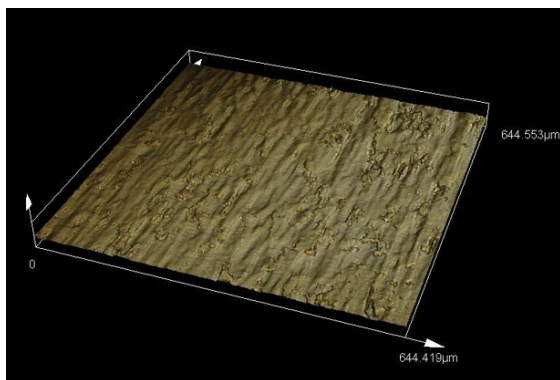


Fig. 12. Surface Roughness Analysis of Ti Gr 2 Markings at 700 kHz: 3D Laser Scanning Microscope Image (x451 Magnification) Showing $R_q = 2.9 \mu\text{m}$.

In Figure 13, the most pronounced colors are captured under the Olympus LEXT laser microscope.

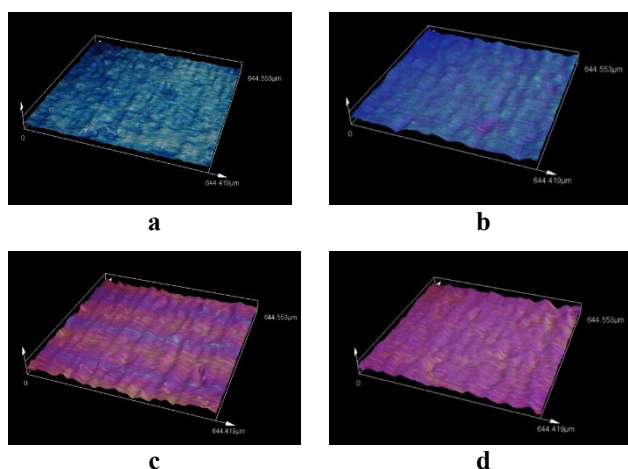


Fig. 13. Color and Roughness Variation on Ti Gr 2 Surface Following Laser Treatment with Specific Parameters.

- $\Delta x = 10 \mu\text{m}$; $\tau = 4 \text{ ns}$; $F = 700 \text{ kHz}$.
a: $P = 10 \text{ W}$; $v = 300 \text{ mm/s}$. **b:** $P = 8 \text{ W}$; $v = 300 \text{ mm/s}$.
c: $P = 10 \text{ W}$; $v = 500 \text{ mm/s}$. **d:** $P = 14 \text{ W}$; $v = 700 \text{ mm/s}$.

This image illustrates the formation and transition of colors, providing insights into both their structure and the details of the color spectrum. Although the color shades differ significantly, the structure and roughness of the Ti surface remains practically unchanged.

IV. CONCLUSION

In this study, we continued our investigation into laser marking treatments for Titanium Grade 2 (Ti Gr 2), focusing on frequencies of 300 kHz and 700 kHz. Our objective was to enhance the global color coding for Ti Gr 2 materials and analyze surface roughness. The data obtained lays the groundwork for achieving desired outcomes across various laser parameters. These findings have significant implications for advancing laser-material interactions and optimizing laser marking processes, particularly for Ti Gr 2, which is widely used in aerospace, medical, and automotive industries. Exploring different frequencies has provided valuable insights into tailoring color spectrum and surface texture, refining laser marking techniques. Further experimentation guided by these insights can enhance control over laser processing of Ti Gr 2, facilitating the production of high-quality components in critical sectors. Our investigation revealed that at 300 kHz, color dynamics and surface roughness are influenced by power and scanning speed, with adjustments in laser parameters showing potential for enhancing desired outcomes. Similarly, at 700 kHz, vivid color tones and similar roughness characteristics were observed, suggesting potential applications in various industries. Future research should explore specific factors influencing observed phenomena within defined frequency ranges, and further investigations into additional frequencies are anticipated to deepen our understanding of Ti Gr 2 laser processing.

REFERENCES

- [1] Romaniuk, R. S., Gajda, J. (April 2013). "Laser Technology and Applications 2012." *International Journal of Electronics and Telecommunications*, 59(2), 195-202.
- [2] Gao, W., Xue, Y., Li, G., Chang, C., Li, B., Hou, Z., Li, K., Wang, J. (2018). "Investigations on the Laser Color Marking of TC4." *International Journal of Electronics and Optoelectronics*, <https://doi.org/10.1016/j.ijleo.2018.12.113>
- [3] Pou, P., Riveiro, A., del Val, J., Comesaña, R., Penide, J., Arias-González, F., Soto, R., Lusquinos, F., Pou, J. (2017). Laser surface texturing of Titanium for bioengineering applications. *Procedia Manufacturing*, 13, 102-107. <https://doi.org/10.1016/j.promfg.2017.09.102>
- [4] Nath, A. (2014). Laser Drilling of Metallic and Nonmetallic Substrates. In: *Laser Precision Microfabrication*. DOI: 10.1016/B978-0-08-096532-1.00904-3.
- [5] Subramonian, S., Kasim, M. S., Ali, M. A. M., Anand, T. J. S., & citi. (2015). Micro Drilling of Silicon Wafer by Industrial CO₂ Laser. *International Journal of Mechanical and Materials Engineering*, 10(1), 1-7. DOI: 10.1186/s40712-015-0029-8.
- [6] Kumar, A., & Kumar, H. (2021). Analysis of material removal of Inconel 718 cylinder using magnetic abrasive finishing process assisted with chemical etching. *Materials Today: Proceedings*. DOI: 10.1016/j.matpr.2021.09.304.
- [7] Hristov, V. N., Lazov, L., Petrov, N. A., Yankov, E. H. (2023). Influence of basic parameters of the laser marking process on stainless steel samples. *Environment Technology Resources Proceedings of the International Scientific and Practical*

- Conference, 3, 311-315. DOI: 10.17770/etr2023vol3.7216.*
- [8] Melo-Fonseca, F., Guimarães, B., Gasik, M., Silva, F. S., & Miranda, G. (2022). Experimental analysis and predictive modelling of Ti6Al4V laser surface texturing for biomedical applications. *Surface Innovations*. DOI: 10.1016/j.surf.2022.102466.
- [9] Henriksen, N. G., Poullos, K., Somers, M. A. J., & Christiansen, T. L. (2023). Impact of laser marking on microstructure and fatigue life of medical grade titanium. *Materials Science and Engineering: A*, 145020. DOI: 10.1016/j.msea.2023.145020.
- [10] Awasthi, A., Kumar, D., & Marla, D. (2023). Understanding the role of oxide layers on color generation and surface characteristics in nanosecond laser color marking of stainless steel. *Optics and Laser Technology*. DOI: 10.1016/j.optlastec.2023.110469.
- [11] Gräf, S., Kunz, C., Undisz, A., Wonneberger, R., Rettenmayr, M., & Müller, F. A. (2019). Mechano-responsive colour change of laser-induced periodic surface structures. *Applied Surface Science*. DOI: 10.1016/j.apsusc.2018.12.051.
- [12] Geng, Y., Li, J., & Lu, C. (2022). Experimental and numerical investigations on color stability of laser color marking. *Optics and Lasers in Engineering*. DOI: 10.1016/j.optlaseng.2022.107225.
- [13] Li, Z., Xu, J., Zhang, D., Xu, Z., Su, X., Jin, Y., Shan, D., Chen, Y., & Guo, B. (2022). Nanosecond pulsed laser cleaning of titanium alloy oxide films: Modeling and experiments. *Journal of Manufacturing Processes*. DOI: 10.1016/j.jmapro.2022.08.033.
- [14] Boyer, R.R. (1996). An overview on the use of titanium in the aerospace industry. *Materials Science and Engineering: A*, 213(1-2), 103-114. DOI: 10.1016/0921-5093(96)10233-1.
- [15] Monogarov, K.A., Pivkina, A.N., Grishin, L.I., Frolov, Yu. V., & Dilhan, D. (2016). Uncontrolled re-entry of satellite parts after finishing their mission in LEO: Titanium alloy degradation by thermite reaction energy. *Acta Astronautica*. DOI: 10.1016/j.actaastro.2016.10.031.
- [16] Arun, A., Lakshmanan, P., Parthiban, K., Kumanan, G., & Arunkumar, L. (2022). Experimental study on laser surface texturing and wear characterization of titanium alloy. *Materials Today: Proceedings*. DOI:10.1016/j.matpr.2022.03.621.
- [17] Morales, M., Munoz-Martin, D., Marquez, A., Lauzurica, S., & Molpeceres, C. (2018). Laser-Induced Forward Transfer Techniques and Applications. In: *Advances in Laser Materials Processing*, Chapter 13, 339-379. DOI: 10.1016/B978-0-08-101252-9.00013-3.
- [18] L. Lyubomir, N. Pavels un D. Hristina, «Laser Marking Methods» *Technology. Resources, (2015), Volume I, 108-115*, pp. 109-112., 2015.
- [19] K. McLAREN, XIII—The Development of the CIE 1976 (L* a* b*) Uniform Colour Space and Colour-difference Formula, vol. 92, *Journal of the Society of Dyers and Colourists*, 1976, pp. 338-341.
- [20] A. J. Arkadiusz, S. Bogusz, K. E. Paweł un A. M. Krzysztof, «The influence of process parameters on the laser-induced coloring» *Applied Physics A volume 115, pages1003–1013 (2014)*, March 2013.
- [21] Lapa, J., Adijans, I., Yankov, E. H., Revalds, R. (2023). "Investigation of Laser Marking and Texturing of Titanium Gr 2 with Fiber Laser." *Environment Technology Resources Proceedings of the International Scientific and Practical Conference, 3, 321-327. DOI: 10.17770/etr2023vol3.7251.*